

Supporting Information

A functionalized membrane for lithium-oxygen batteries to suppress the shuttle effect of redox mediators

Zi-Fang Chen,^{‡a} Xiaodong Lin,^{‡a} Hui Xia,^a Yuhao Hong,^a Xiaoyu Liu,^a Senrong Cai,^a Jia-Ning Duan,^a Junjie Yang,^a Zhiyou Zhou,^a Jeng-Kuei Chang,^b Mingsen Zheng^{*a} and Quanfeng Dong^{*a}

^aState Key Laboratory of Physical Chemistry of Solid Surfaces, Department of Chemistry, College of Chemistry and Chemical Engineering, Collaborative Innovation Center of Chemistry for Energy Materials (*iChEM*), Xiamen University, Xiamen, Fujian 361005, China

^bDepartment of Materials Science and Engineering, National Chiao Tung University, Hsinchu, Taiwan.

[‡]These authors contributed equally to this work.

*Correspondence: qfdong@xmu.edu.cn, mszheng@xmu.edu.cn

Supplementary Experimental Section

X-ray diffraction (XRD) measurements

The Li-O₂ batteries were disassembled in glovebox and the discharged/recharged oxygen electrodes were washed with anhydrous DME several times and dried under vacuum. Then, the dried electrodes were placed in a commercial fluted glass and sealed with a kapton polyimide film before taking it out of the glovebox. Further, the sealed electrodes were detected by using a Rigaku Ultima IV X-ray diffractometer Cu K α radiation ($\lambda=1.5418 \text{ \AA}$) at a scan angle range of 20-60°. Nafion sample was dropped onto a glass slide and dried before test. The NPG, PEO, Nafion and RGO samples were measured directly in air.

Scanning electron microscopy (SEM) measurements

The discharged/recharged oxygen electrodes and Li anodes used for SEM tests were treated similarly to that of XRD measurements. The dried electrodes were immobilized on a SEM sample stage and enclosed into a sealed bag before being exposed to air, the sample stage was transferred to the sample chamber and pumped immediately after being taken out from the sealed bag. Then, the nanostructures and surface morphologies of the discharged/recharged oxygen electrodes and Li anodes were investigated by using a Zeiss SIGMA microscope. The NPG membrane sample was investigated directly without seal transfer procedure.

X-ray photoelectron spectroscopy (XPS) measurements

The Li anodes used for XPS measurements were treated similarly to that of XRD measurements. The dried Li anodes were transferred into the XPS chamber by using a commercial air-isolating container. Then, the XPS measurements were performed on PHI 5000 Versa Probe II (UHVAC-PHI) using monochromatic Al K α (1486.6 eV) X-ray source at 24 W and 16 KV with a beam spot size of 100 μm . The binding energies were referenced to the C 1s line at 284.6 eV from adventitious carbon. Depth profiling was fulfilled using Ar ion sputtering in the x-y scan mode at ion acceleration of 2 kV and ion beam current of 2 μA over an area of 2 \times 2 mm². The NPG membrane and PEO samples used for XPS measurements were prepared by the usual way.

Raman spectra measurements

The discharged oxygen electrodes used for Raman spectra measurements were treated similarly to that of XRD measurements. The dried electrodes were loaded into a gas-tight Raman cell with a quartz window in glovebox before test. Then, the Raman spectra was recorded on a XploRA Confocal Raman Microscope (Jobin Yvon-Horiba, France) with an excitation wavelength of 532 nm. The Nafion and Nafion-PEO samples were dropped onto a glass slide and dried before test.

In-situ differential electrochemical mass spectrometry (DEMS) measurements

For *in-situ* DEMS measurements, the Swagelok-type Li-O₂ batteries were linked to a commercial mass spectrometer (MSD, Agilent, 5975C) with EI source. For charge process, the residual gas in the Swagelok-type Li-O₂ cell was purged by high-purity He. Then, He carrier gas was purged into the Li-O₂ cell to push the generated O₂ and other gas toward the MSD. As for the discharge process, 2 % O₂/Ar mixed gas was used as both reactant gas to offer an oxygen reduction reaction and carrier gas to push the generated gas toward the MSD. The quantification of gas (CO₂, O₂ and H₂) was calibrated by a standard gas. The flow rate of the carrier gas was 8 mL min⁻¹.

Table S1. Raman shift of the bonds in PEO and Nafion.

Assignment	PEO/cm ⁻¹	Nafion/cm ⁻¹
CH ₂ stretching	841.1	/
Coupled C-O stretching/CH ₂ rocking	856.3	/
Coupled C-O-C stretching/CH ₂ rocking	1060.5	/
Coupled C-C stretching/CH ₂ rocking	1123	/
Coupled C-C/C-O-C stretching	1139	/
CF ₂ stretching	/	730.6
C-S stretching	/	802
S-O stretching	/	1057

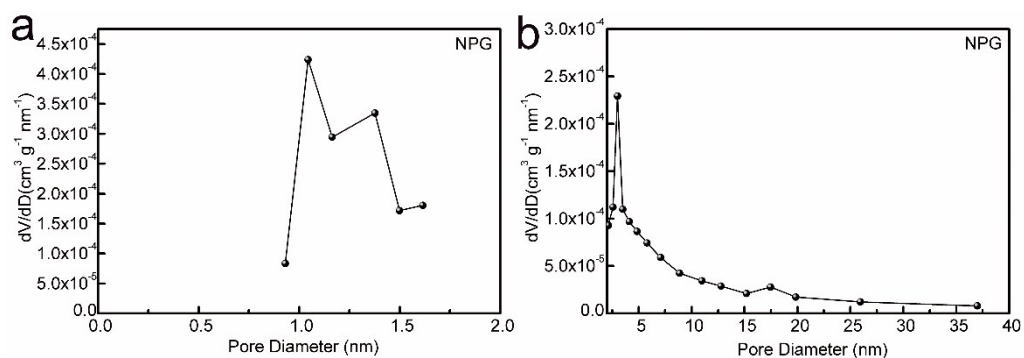


Figure S1. BJH pore size distributions of NPG membrane in a range of (a) 0~2 nm and (b) >2 nm.

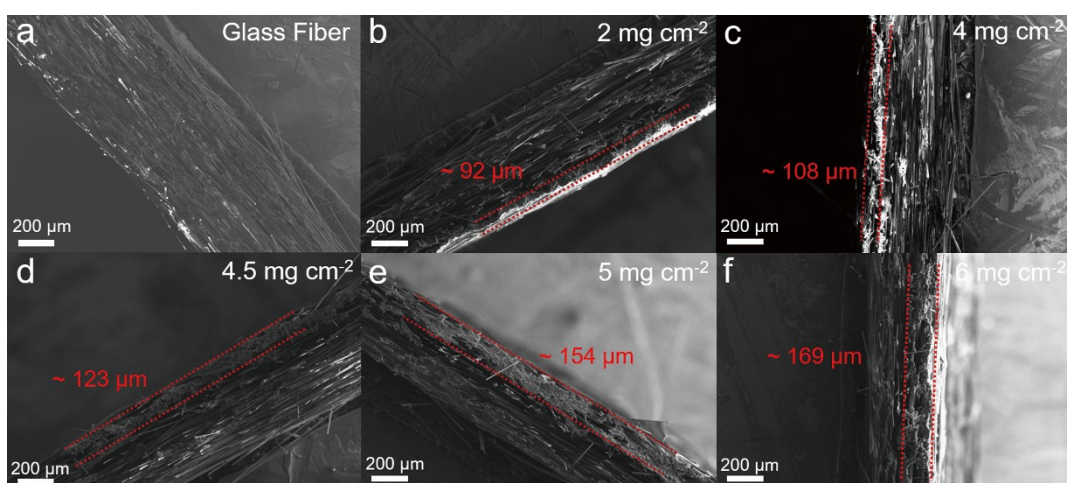


Figure S2. SEM images of the GF (a) and NPG membrane with loading mass of 2 mg cm⁻² (b), 4 mg cm⁻² (c), 4.5 mg cm⁻² (d), 5 mg cm⁻² (e), and 6 mg cm⁻² (f).

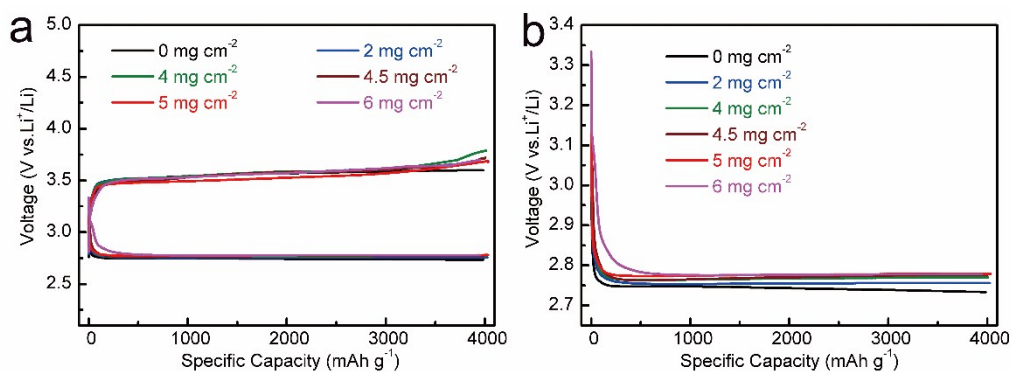


Figure S3. (a) The discharge/charge profiles of the LiI-based Li-O₂ batteries with different loading mass of NPG materials. (b) The enlarged image of the discharge curves corresponding to (a).

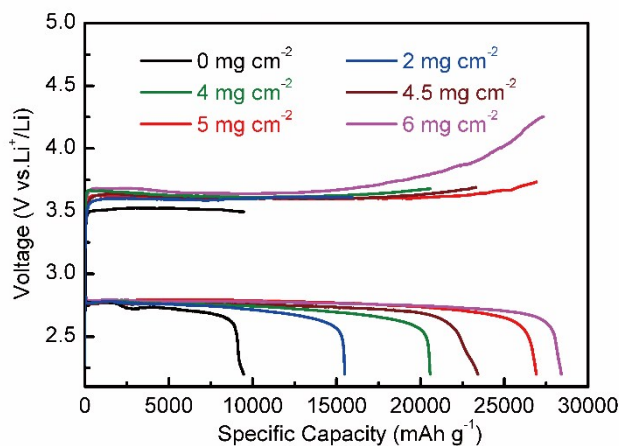


Figure S4. The full discharge/charge profiles of the LiI-based Li-O₂ batteries with different loading mass of NPG materials.

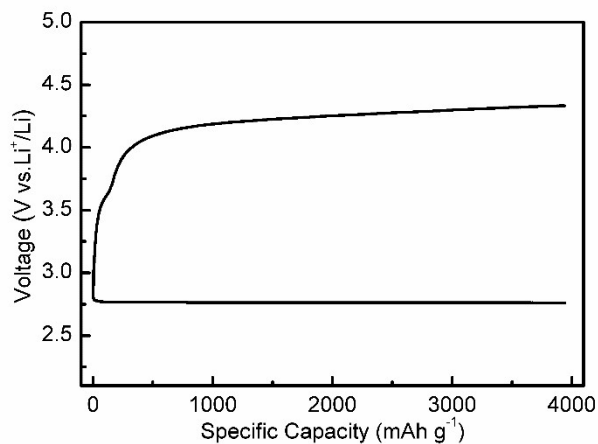


Figure S5. The discharge/charge profile of the LiI-free Li-O₂ battery without NPG membrane at a current density of 500 mA g⁻¹ with a high cutoff capacity of 4000 mAh g⁻¹.

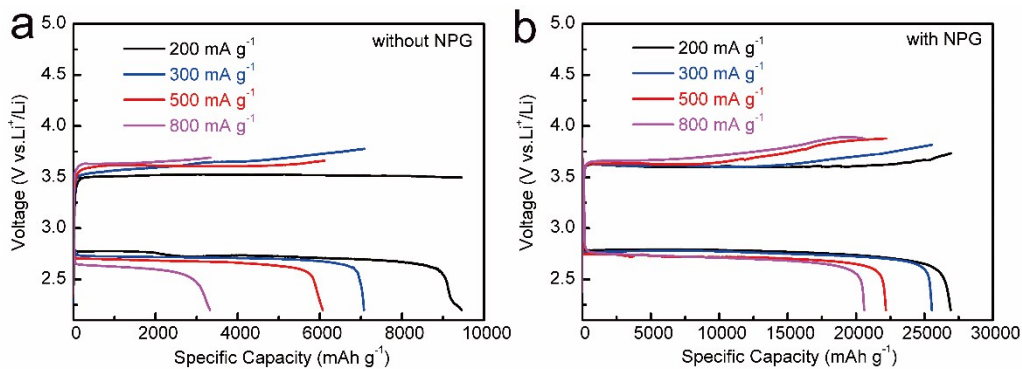


Figure S6. The full discharge/charge curves of the LiI-based Li-O₂ batteries (a) without and (b) with NPG membrane at various current densities (200 mA g⁻¹, 300 mA g⁻¹, 500 mA g⁻¹, 800 mA g⁻¹).

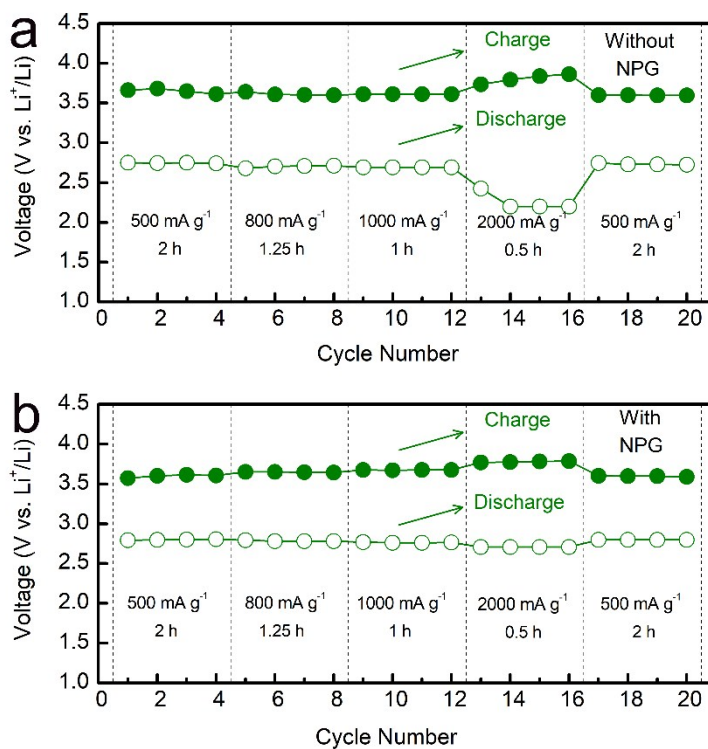


Figure S7. Discharge/charge terminal voltages of the LiI-based Li-O₂ batteries (a) without and (b) with NPG membrane at various current densities (500 mA g⁻¹, 800 mA g⁻¹, 1000 mA g⁻¹, 2000 mA g⁻¹) with a cutoff capacity of 1000 mAh g⁻¹.

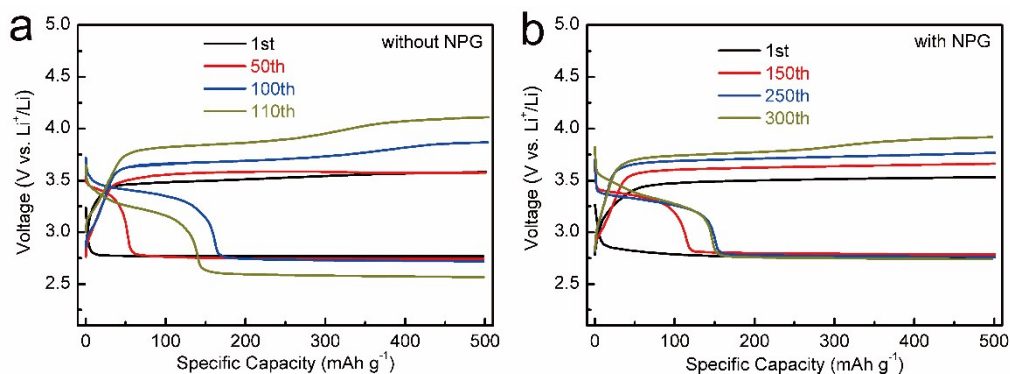


Figure S8. Discharge/charge curves of the LiI-based Li-O₂ batteries (a) without and (b) with NPG membrane at a current density of 500 mA g⁻¹ with a cutoff capacity of 500 mA h g⁻¹.

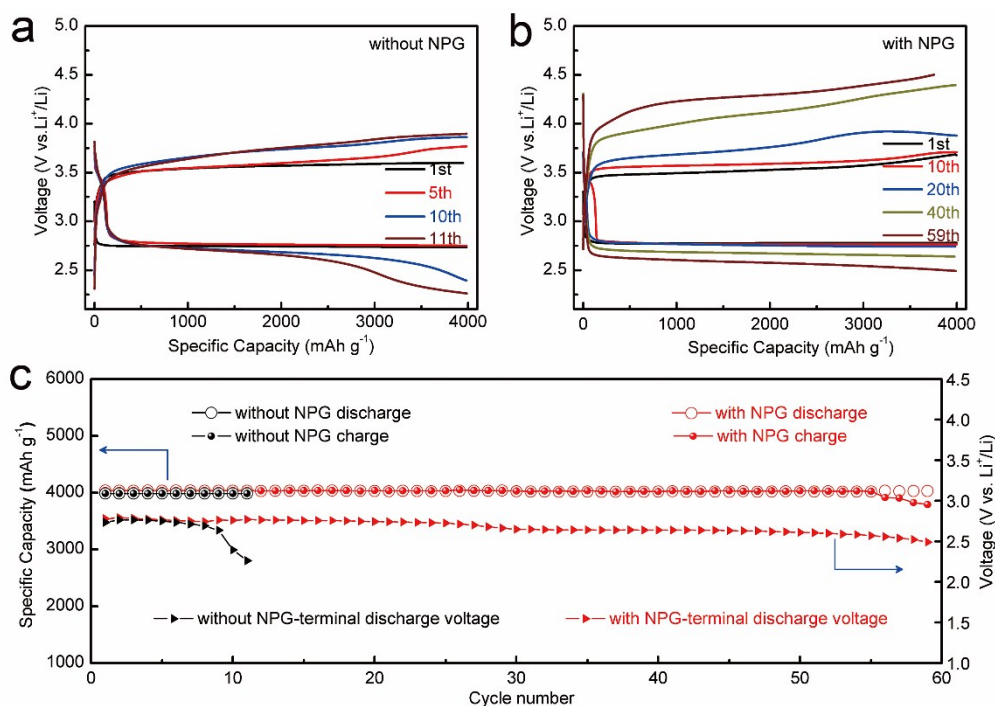


Figure S9. Discharge/charge curves of the LiI-based Li-O₂ batteries (a) without and (b) with NPG membrane at a current density of 500 mA g⁻¹ with a high cutoff capacity of 4000 mA h g⁻¹. (c) Cycling stability and the corresponding terminal discharge voltage of the LiI-based Li-O₂ batteries with and without NPG membrane at a current density of 500 mA g⁻¹ with a high cutoff capacity of 4000 mA h g⁻¹.

Table S2. Comparison of the performance of our work with related studies about inhibiting the shuttle effect of redox mediators.

Material	Electrolyte	Thickness/ Mass of interlayer	Mass of active material (mg cm ⁻²)	Voltage platform (V) (Discharge/ Charge)	Discharge capacity (mAh g ⁻¹)	Cycling number (without/with)	Current density (mA g ⁻¹)/fixed capacity (mAh g ⁻¹)	Ref
NPG Membrane	50 mM LiI + 0.5 M LiTFSI in DMSO	5 mg cm ⁻² (~154 μm)	0.2~0.5 (RGO)	2.77/3.5	~26917 (12.38 mAh cm ⁻²)	123 / 472 11 / >59	500 / 500 500 / 4000	This work
Self- defense RM (InI ₃)	16.7 mM InI ₃ + 0.5 M LiClO ₄ in DMSO	~	0.5 (MWCNTs)	~2.8/~3.5	~	< 10 / >40	1000 / 1000	<i>Energy Environ. Sci.</i> , 2016, 9 , 1024- 1030.
Al ₂ O ₃ /PVdF-HFP	50 mM TEMPO + 1 M LiClO ₄ in TEGDME	25 μm	0.8 (Super-P)	~2.65/~3.65	~	60 / 175	0.125 mA cm ⁻² / 0.5 mAh cm ⁻²	<i>Adv. Mater.</i> , 2016, 28 , 857-863.
GPDL	0.5 M LiBr + 0.5 M LiTFSI in DEGDME	30 μm	GDL, d=12 mm	~2.75/3.4	~	15 / >150	0.15 mA cm ⁻² / 0.6 mAh cm ⁻²	<i>Adv. Energy Mater.</i> , 2018, 8 , 1702258.
LICGC	Cathode: 0.2 M DMPZ + 1M LiTFSI in TEGDME Anode: 1M LiTFSI in TEGDME:FE C=4:1	150 μm	0.3 (CNT/GDL)	~2.75/~3.2	~	25 / >60	400 / 2000	<i>Adv. Energy Mater.</i> , 2017, 7 , 1701232.
GO membrane	0.2 M DMPZ + 1M LiTFSI in TEGDME	0.01 mg cm ⁻²	0.15 (CNT film)	2.68/3.21	~	40 / >80	0.15 mA cm ⁻² / 0.5 mAh cm ⁻²	<i>Small</i> , 2018, 14 , 1801456.

Li ⁺ -Nafion	50 mM DBBQ + 50 mM DMPZ + 1 M LiTFSI in TEGDME	Nafion 117 membrane	0.2 (RuO ₂)	~2.8/~3.2	5800	~ / 60	250 / 1000	<i>J. Mater. Chem. A</i> , 2018, 6 , 9816-9822.
PPy film	0.2 M Lil + 1 M LiTFSI in DMSO	20~30 μm	Carbon Paper, d=10 mm	2.7/3.6	~	6 / 17	0.1 mA cm ⁻² / 0.3 mAh cm ⁻²	<i>APL Mater.</i> , 2018, 6 , 047704.
(MOF)-based separator	25 mM DBBQ + 50 mM TTF + 1 M LiTFSI in TEGDME	1 mg cm ⁻²	0.25~0.35 (SWCNT)	~2.7/~3.4	3.2 mAh cm ⁻²	33 / 120	1000 / 2500	<i>ACS Energy Lett.</i> , 2018, 3 , 463-468.
PEDOT:PSS-coated separator	0.2 M DMPZ + 1M LiTFSI in DEGDME	20 μm	GDL	~2.75/~3.25	~	~ / >25	0.052 mA cm ⁻² / 0.5 mAh cm ⁻²	<i>Adv. Energy Mater.</i> , 2017, 7 , 1602417.
QSPE	0.4 M TEMPO + 1M LiTFSI in TEGDME	140 μm	1.0 (Super-P)	~2.7/3.5	~	150 / >200	100 / 500	<i>Adv. Mater. Interfaces</i> , 2017, 4 , 1700693.

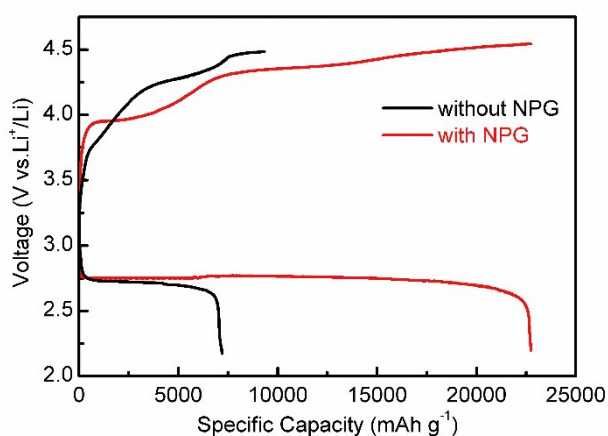


Figure S10. The full discharge/charge profiles of the LiI-free Li-O₂ batteries with and without NPG membrane at a current density of 200 mA g⁻¹ in a voltage window between 2.2 and 4.5 V.

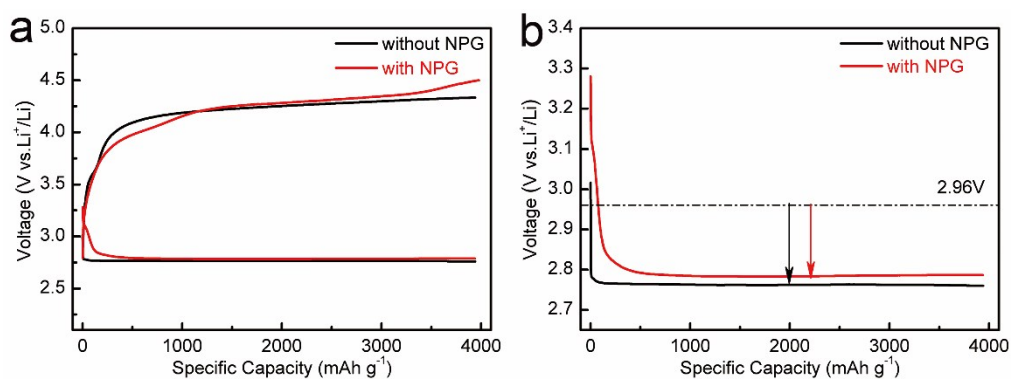


Figure S11. (a) The discharge/charge profiles of the LiI-free Li-O₂ batteries with and without NPG membrane at a current density of 500 mA g⁻¹ with a high cutoff capacity of 4000 mA h g⁻¹. (b) The enlarged image of the discharge curves corresponding to (a).

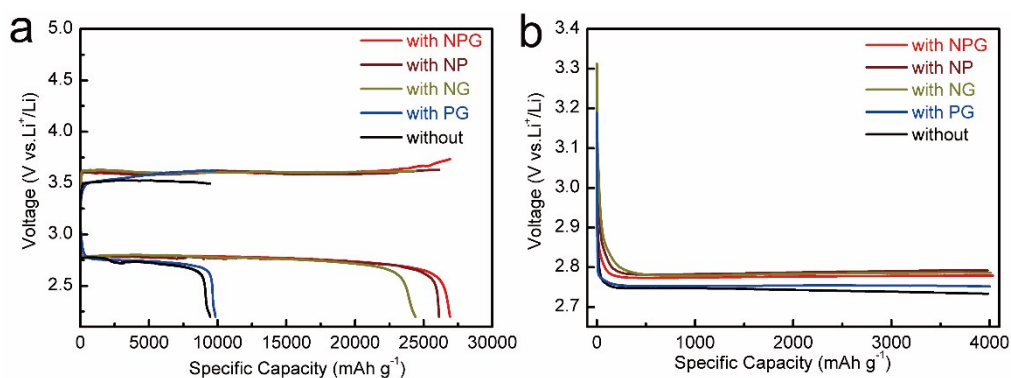


Figure S12. (a) The full discharge/charge profiles of the LiI-based Li-O₂ batteries without and with different kinds of membranes at a current density of 200 mA g⁻¹ in a voltage window between 2.2 and 4.5 V. (b) The discharge curves of the LiI-based Li-O₂ batteries without and with different kinds of membranes at a current density of 500 mA g⁻¹ with a high cutoff capacity of 4000 mA h g⁻¹.

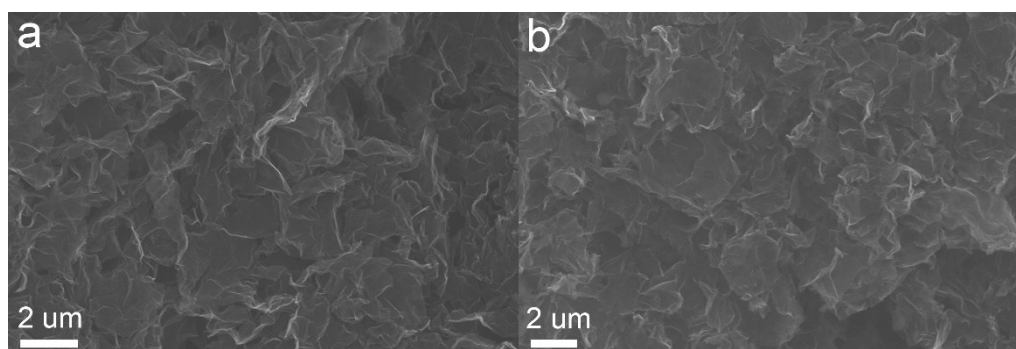


Figure S13. SEM images of the cathode surface of the LiI-based Li-O₂ batteries (a) without and (b) with NPG membrane after charge.

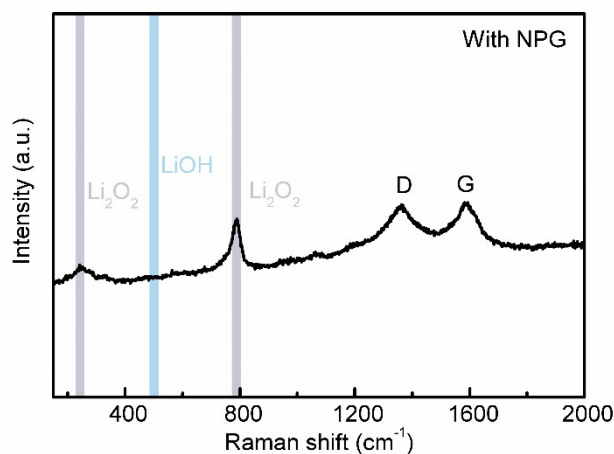


Figure S14. Raman spectra of the oxygen cathode extracted from NPG membrane-based Li-O₂ battery after discharge.

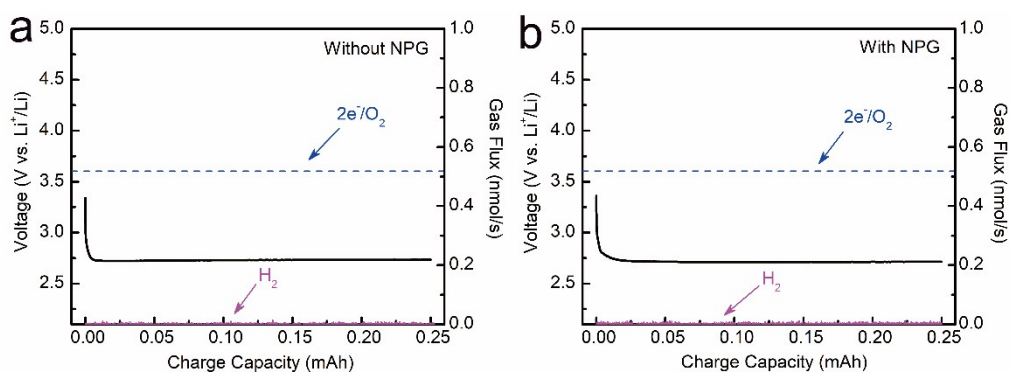


Figure S15. Galvanostatic discharge (at a current of 0.1 mA) profile and corresponding H₂ evolution rates of the LiI-based Li-O₂ batteries (a) without and (b) with NPG membrane.

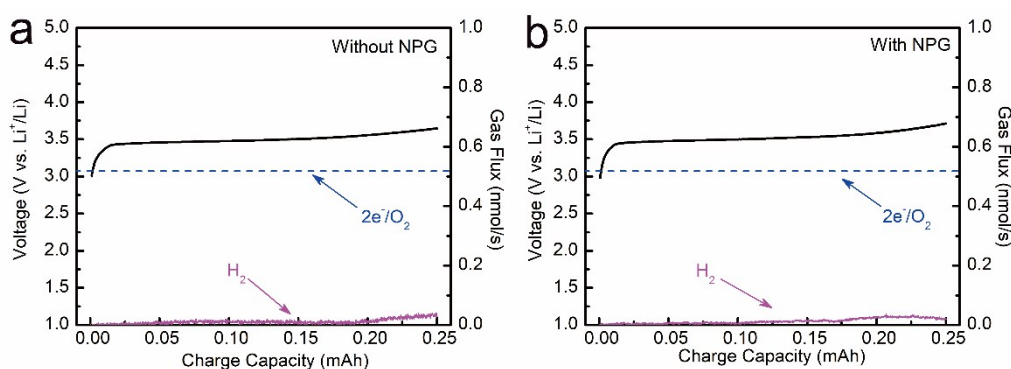


Figure S16. Galvanostatic charge (at a current of 0.1 mA) profile and corresponding H₂ evolution rates of the LiI-based Li-O₂ batteries (a) without and (b) with NPG membrane.

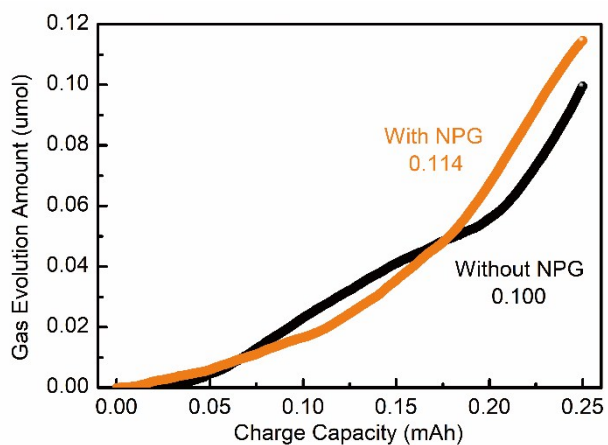


Figure S17. H₂ evolution amount during charge process in the LiI-based Li-O₂ battery with and without NPG membrane that is related to Figure S16.

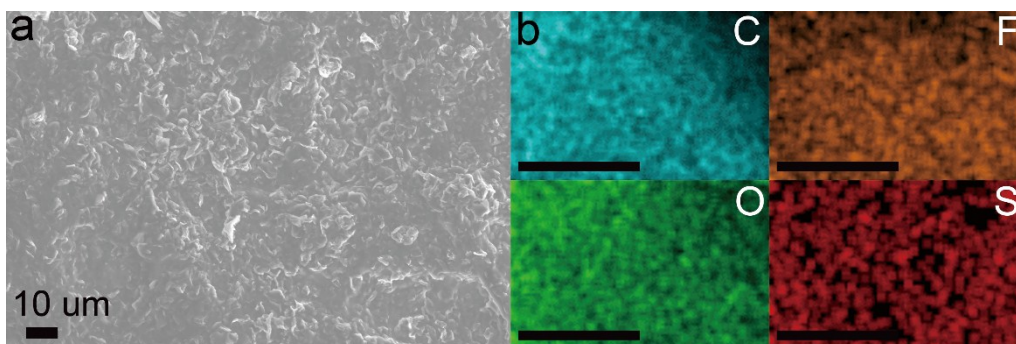


Figure S18. (a) SEM image and (b) EDX maps (scale: 5 μm) of the NPG membrane after 1st cycle with a high cutoff capacity of 4000 mA h g⁻¹.

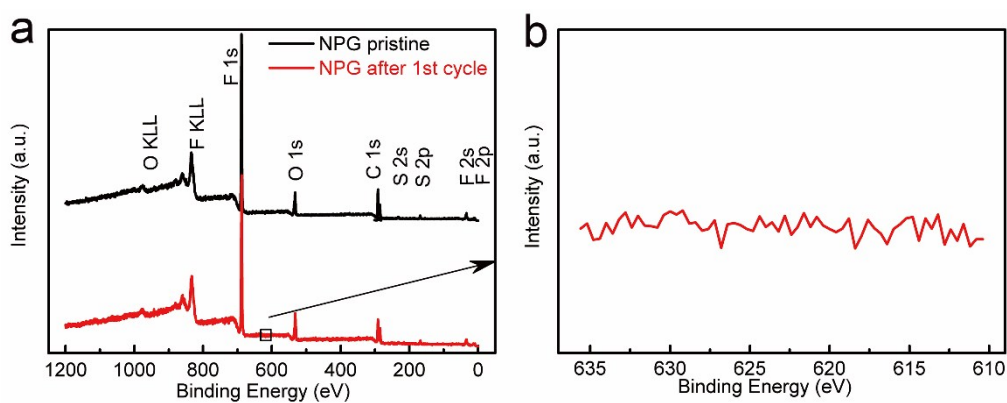


Figure S19. (a) The XPS survey spectra of the NPG membrane before and after the first cycle. (b) The I 3d XPS spectra of the NPG membrane after the first cycle.

Table S3. Comparison of the elemental atomic ratio of the NPG membrane before and after 1st cycle.

Elements	Pristine NPG membrane Atomic ratio (%)	NPG membrane after 1 st cycle Atomic ratio (%)
F	47.7	48.3
C	35.7	37.9
O	14.6	12.5
S	2.0	1.3

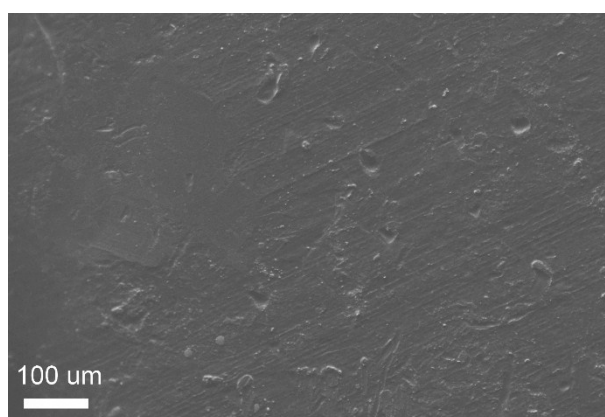


Figure S20. SEM image showing the surface of a fresh Li metal anode.

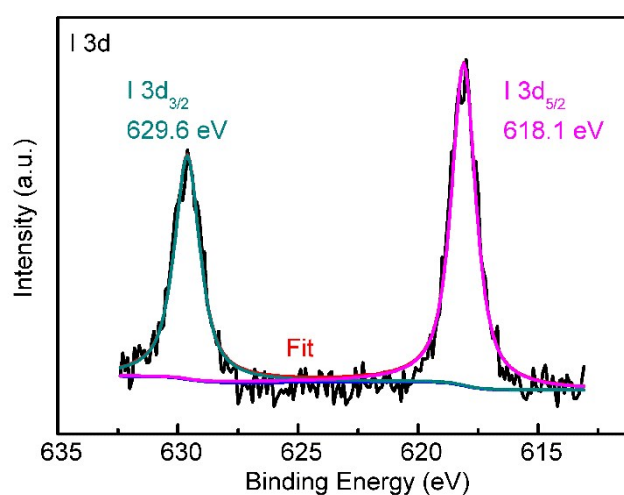


Figure S21. The I 3d XPS spectra of the Li anode surface without NPG membrane after 25 cycles.